nitrogen

MDPI

Article

Determination of Optimal Nitrogen Application Rates to Enhance Heat Stress Tolerance in Autumn Radish (*Raphanus sativus* L.) Using OJIP Transient Analysis

Tae Seon Eom [1], Tae Wan Kim [1,*] and Sung Yung Yoo [2,*]

[1] School of Plant Resources and Landscape Architecture, Hankyong National University, Anseong 17579, Republic of Korea; ymh5240@hknu.ac.kr
[2] Institute of Ecological Phytochemistry, Hankyong National University, Anseong 17579, Republic of Korea
* Correspondence: taewkim@hknu.ac.kr (T.W.K.); lsn136@hknu.ac.kr (S.Y.Y.); Tel.: +82-10-6292-3896 (T.W.K.); +82-10-4938-6825 (S.Y.Y.)

Abstract

High-temperature stress severely reduces the photosynthetic efficiency of radish (*Raphanus sativus* L.), a cool-season crop. This study evaluated five nitrogen (N) levels {0 N, 0.5 N, 1 N (234 kg urea ha^{-1}, based on RDA), 2 N, and 4 N} through an open-field experiment under high-temperature stress conditions. Analysis of OJIP transients revealed that high temperatures severely inhibited photosynthetic capacity in the 0 N, 0.5 N, and 4 N treatment groups. These groups exhibited a simultaneous increase in K and J-steps, signifying electron transport bottlenecks and structural damage to the oxygen-evolving complex (OEC). Consequently, energy absorption and trapping decreased, while heat dissipation increased. In contrast, the 2 N treatment maintained superior F_m(maximum fluorescence) and energy flux, demonstrating enhanced photosynthetic resilience. However, despite improved photosynthetic stability, the 2 N group did not show a significant increase in yield compared to the 0.5 N or 1 N treatment groups. These results suggest that photosynthetic protection under heat stress does not necessarily guarantee higher yields, highlighting the need to identify optimal fertilization points for sustainable production. Overall, the findings of this study provide fundamental data for strategic nitrogen management in open-field radish cultivation to mitigate the impacts of increasing climatic instability.

Keywords: radish; OJIP transient; nitrogen nutrition; heat stress; abiotic stress tolerance

Check for updates

Academic Editors: Nasratullah Habibi and Francisco Padilla

Received: 12 March 2026
Revised: 10 April 2026
Accepted: 16 April 2026
Published: 23 April 2026

Copyright: © 2026 by the authors. Licensee MDPI, Basel, Switzerland. This article is an open access article distributed under the terms and conditions of the Creative Commons Attribution (CC BY) license.

1. Introduction

Radish (*Raphanus sativus* L.) is a major root vegetable valued for its edible leaves and roots. It is widely cultivated and consumed worldwide owing to its short growth cycle and high nutritional value [1]. As a cool-season crop, radish is primarily cultivated during the spring and fall in many regions [2]. Radishes have diversified into various cultivars in response to regional climatic characteristics, soil environments, and consumer preferences. In East Asia, specifically Korea, China, and Japan, cultivars characterized by large, elongated white roots predominate, holding significant economic importance and distinguishing them from the smaller varieties common in Western countries [3,4]. However, the increasing frequency of abiotic stress driven by recent extreme weather events has emerged as a critical constraint limiting crop growth duration, yield, and quality [5]. Radish is particularly vulnerable to high-temperature stress, which impairs the photosynthetic apparatus by reducing chlorophyll content and downregulating genes associated

with light-harvesting complexes [6]. Such a reduction in photosynthesis, coupled with accelerated respiration under heat, leads to the excessive consumption of photoassimilates. These metabolic imbalances interfere with the translocation of nutrients to the underground organs, ultimately causing productivity losses through the inhibition of root thickening and reduced starch accumulation [7]. To mitigate these environmental constraints, plant nutrient management has been employed as a fundamental strategy to modulate physiological responses [8]. Nitrogen (N), in particular, is a vital macronutrient that serves as the structural backbone for biological compounds, including amino acids, proteins, and nucleic acids [9]. Beyond its structural role, a broad spectrum of physiological traits such as root architecture development, growth rate, the onset of chlorophyll senescence, photosynthetic capacity, and environmental stress resilience is intricately linked to nitrogen uptake and use efficiency [10–12]. Abnormally high temperatures during the root enlargement stage impair the metabolic mechanisms of radish, leading to stunted growth and reduced starch accumulation [13]. Under heat stress, plants induce heat shock proteins (HSPs) and accumulate substances like proline to maintain cellular homeostasis as part of a well-documented molecular defense mechanism [14]. Since the synthesis of these protective proteins and substances like proline demands a substantial allocation of nitrogen resources, nitrogen availability is considered a critical determinant of the physiological buffering capacity against high-temperature stress [15,16]. However, the efficacy of nitrogen fertilization varies according to stress intensity and crop growth stages; furthermore, imbalanced nitrogen supply, whether excessive or deficient, can exacerbate stress susceptibility [12,17,18]. Therefore, determining the optimal nitrogen application rate to maintain the physiological homeostasis of radish under climate-driven complex environmental stresses is imperative for ensuring stable crop production.

OJIP (Origin-J-I-P) transient analysis, a specialized form of chlorophyll *a* fluorescence measurement, is a technique that quantifies the stepwise transitions of the photosynthetic electron transport chain based on fluorescence phenomena occurring within 2 ms [19,20]. The OJIP transient reflects the photochemical quantum yield and electron transport capacity of Photosystem II (PSII). By analyzing the fluorescence kinetics at each stage, the electron transfer efficiency between photosynthetic apparatuses and the overall physiological vitality of the plant can be precisely assessed [21,22]. Various performance indices (PI) derived from this analysis have been established as robust indicators for quantifying plant resilience to abiotic stresses, such as high light, drought, extreme temperatures (heat and cold), and nutrient deficiencies [23–25]. Furthermore, as a non-destructive approach, this technique enables longitudinal (time-series) monitoring of the same individual, facilitating a comprehensive analysis of dynamic physiological shifts as stress progresses [26,27].

In a previous study, it was confirmed that a fertilization level of 0.5 N maintained standard growth while reducing environmental loads [28]. However, as high-temperature events become more frequent due to climate change, it has not yet been investigated whether such low-input fertilization is sufficient to sustain the physiological defense mechanisms, particularly PSII efficiency. Therefore, this study aims to analyze the physiological responses of Korean fall radish under various N conditions during heat stress. By identifying the optimal nitrogen application levels that maximize tolerance to heat stress ranging from low-input to excessive levels (4 N), this study aims to suggest efficient fertilization standards for stable crop production under unstable climatic environments.

2. Materials and Methods

2.1. Plant Materials and Experimental Design

This study was conducted in an open field located in Anseong, Gyeonggi-do, South Korea (37°00′ N, 127°19′ E). The fall radish cultivar 'Tongil-kimjang' (Kyung Nong Co.,

Ltd., Seoul, Republic of Korea) was used as the experimental material. The experimental area was divided into 1 m × 2 m plots, arranged in a completely randomized design (CRD) with three replicates. To ensure independent and controlled growth environments, each plot was physically isolated by barriers, effectively minimizing cross-interference and nutrient leaching between treatments. Before sowing, all plots were mulched with black polyethylene film to suppress weed growth and maintain soil moisture. The soil at the experimental site was classified as loam; its physicochemical properties are summarized in Table 1.

Table 1. Chemical properties of soil prior to fertilizer application.

Soil Texture	pH	Organic Matter	Total Kjeldahl Nitrogen	Av. P_2O_5	K^+	Ca^{2+}	Mg^{2+}
	(1:5)	(g kg^{-1})	(mg kg^{-1})	(mg kg^{-1})		($cmol_c$ kg^{-1})	
Loam	5.33	9.80	839.3	398.7	0.66	3.62	0.22

Data source: Modified from [28].

2.2. Cultivation and Fertilization Management

Radish seeds were sown at a density of 25 cm × 30 cm (12 plants per plot), with three seeds per hole, and later thinned to one healthy plant at 14 days after sowing (DAS). Consequently, each treatment comprised a total of 36 individual plant replicates (n = 36) across the three plots to ensure high statistical reliability. Each nitrogen treatment was performed in triplicate to ensure statistical reliability. Urea was selected as the primary nitrogen source, reflecting its widespread use in South Korean agricultural practices. To evaluate the regulatory role of nitrogen (N) in radish growth and its potential to mitigate heat stress, urea was administered at five distinct levels: 0 (0 N), 117 (0.5 N), 234 (1 N), 468 (2 N), and 936 (4 N) kg urea ha^{-1}. The 1 N level (234 kg urea ha^{-1}) was established based on the standard fertilizer application guidelines provided by the Rural Development Administration (RDA) of South Korea (Table 2). All plots received a basal application of compost, phosphorus (51 kg P_2O_5 ha^{-1}), potassium (81 kg KCl ha^{-1}), lime (2000 kg ha^{-1}), and borax (20 kg ha^{-1}). Urea and potassium were applied through a basal application followed by two subsequent top-dressings at 21 and 32 DAS. For each top-dressing, a hole approximately 2–3 cm deep was made between the plants, and the fertilizer was applied into the hole to prevent direct contact with the plants and minimize nutrient loss. The experiment was conducted under rainfed conditions, and the crops were harvested on 12 November 2021(70 DAS).

Table 2. Summary of the treatments in this study with four different concentrations of urea.

Treatment	Compost (kg ha^{-1})	Basal Application (kg ha^{-1})		First Top-Dressing (21 DAS) (kg ha^{-1})		Second Top-Dressing (32 DAS) (kg ha^{-1})	
		N	K	N	K	N	K
0 kg urea ha^{-1} (0 N)	15,000	0	62	0	56.5	0	56.5
117 kg urea ha^{-1} (0.5 N)	15,000	42	62	37.5	56.5	37.5	56.5
234 kg urea ha^{-1} (1 N)	15,000	84	62	75	56.5	75	56.5
468 kg urea ha^{-1} (2 N)	15,000	168	62	150	56.5	150	56.5
936 kg urea ha^{-1} (4 N)	15,000	336	62	300	56.5	300	56.5

2.3. Environmental Conditions

Daily meteorological data, including air temperature and soil water content (SWC), were monitored using an automated weather station (WatchDog 2900ET; Spectrum Technologies, Inc., Aurora, IL, USA) installed at the experimental site (Figure 1). During the

critical growth stages, particularly starting from 40 days after sowing (DAS), the plants were exposed to recurring high-temperature stress, with daily maximum temperatures frequently exceeding 30 °C and peaking at 37.5 °C. To isolate the effects of thermal stress from those of water deficit, SWC was maintained within a stable range of 25–35% throughout the study period. To monitor the representative soil moisture conditions of the experimental field, SWC was measured in the 0.5 N, 1 N, and 2 N plots. Representative soil moisture was determined by averaging SWC measurements from the 0.5 N, 1 N, and 2 N plots.

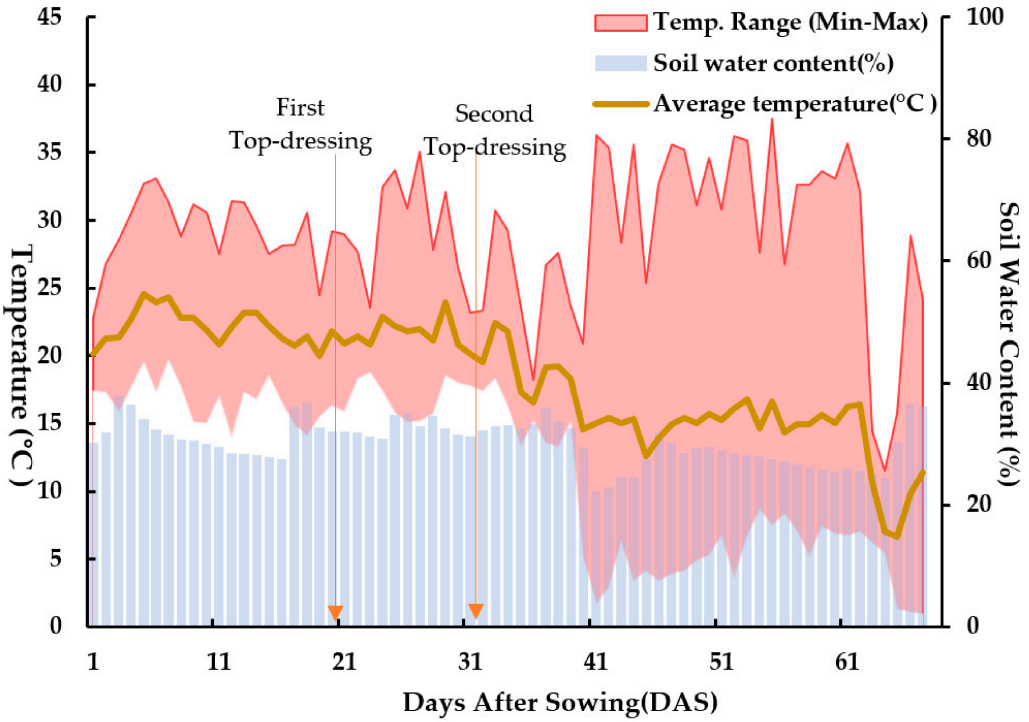


Figure 1. Daily changes in air temperature and soil water content (SWC) during the experimental period, monitored by an automated weather station.

2.4. Chlorophyll a Fluorescence Measurements and JIP-Test

Chlorophyll *a* fluorescence transients (OJIP) were measured using a portable fluorometer (FluorPen FP 100; Photon Systems Instruments, Drásov, Czech Republic). Monitoring began three weeks after sowing (25 September) and continued until 2 November (10 days before harvest). While measurements were generally taken weekly, intensive monitoring occurred every two days for one week following each top-dressing (25 September and 12 October) to capture the acute mitigative effects of nitrogen under heat stress, totaling 12 collection points. All measurements were conducted between 10:00 and 14:00 h, coinciding with peak heat stress. Prior to each measurement, the target leaves were dark-adapted for 30 min using specialized leaf clips to ensure the complete reduction of the PSII reaction centers. Subsequently, OJIP transients were induced by a saturating red-light pulse of 3000 μmol m^{-2} s^{-1}. The recorded data were analyzed through the JIP-test according to the protocols defined by Stirbet and Govindjee (2011) [21], with six biological replicates performed for each treatment to ensure statistical reliability (Table 3).

Table 3. Summary of JIP-test parameters, formulae, and their physiological meanings used for the analysis of chlorophyll *a* fluorescence transients (OJIP) (adapted from [21]).

Data extracted from the recorded fluorescence transient O-J-I-P	
F_O	Fluorescence at the O-step (50 μs)
$F_J \equiv F_{2m}$	Fluorescence at the J-step (2 ms)
$F_I \equiv F_{30ms}$	Fluorescence at the I-step (30 ms)
$F_P \equiv (F_M)$	Maximal fluorescence at the peak P
$F_V \equiv F_M - F_O$	Maximal variable fluorescence
$V_J = (F_J - F_O)/(F_M - F_O)$	Relative variable fluorescence at the J-step
$V_I = (F_I - F_O)/(F_M - F_O)$	Relative variable fluorescence at the I-step
$F_V/F_M = 1 - F_O/F_M$	Maximum quantum yield of primary PSII photochemistry
Phenomenological energy fluxes (per excited cross-section—CS)	
ABS/CS	Absorption flux per CS (at $t = 0$)
$TR_O/CS = \varphi_{P_O}(ABS/CS)$	Trapped energy flux per CS (at $t = 0$)
$ET_{2O}/CS = \varphi_{E_O}(ABS/CS)$	Electron transport flux per CS (at $t = 0$)
$RE_{1O}/CS = \varphi_{RE_{1O}}(ABS/CS)$	Electron transport flux until PSI acceptors per CS (at $t = 0$)
$DIO/CS = (ABS/CS) - (TR_O/CS)$	Dissipated energy flux per CS (at $t = 0$)

2.5. Statistical Analysis

Data were analyzed using R (version 4.2.1; R Core Team, 2022). Normality and homogeneity of variances were verified using Shapiro–Wilk and Levene's tests, respectively. For datasets meeting these assumptions, a one-way analysis of variance (ANOVA) was performed, followed by Duncan's Multiple Range Test (DMRT) for post hoc comparisons. For non-conforming datasets, the Aligned Rank Transform (ART) was employed via the ARTool package, with Fisher's Least Significant Difference (LSD) adjustment (using the art.con function) for *post hoc* analysis. All statistical significance was determined at $p < 0.05$.

3. Results and Discussions

3.1. Study on Emergence and Growth Responses to Different Urea Application Levels

Emergence rates remained consistently high (>90%) from the 0 N level to the 2 N level; the 4 N level led to a sharp decline to approximately 60%, accompanied by a substantial increase in variance (Figure 2). This significant inhibition of emergence at the 4 N level is attributed to ammonia toxicity resulting from urea hydrolysis (Figure A1). According to a previous study, although ammonia volatilization for the 4 N level was not directly measured, it was reported that the 2 N level produced approximately 0.9 kg NH_3 ha^{-1} day^{-1} of ammonia on the third day after sowing [28] (see Equation (A1)). While a positive correlation between urea application rates and ammonia emissions is well established, recent analyses further specify that this relationship is nonlinear; ammonia volatilization increases exponentially as nitrogen input exceeds optimal levels [29]. Thus, the 4 N treatment likely triggered a disproportionate surge in ammonia concentration rather than a simple linear doubling of 2 N emissions. Existing literature confirms that ammonia volatilized from urea significantly suppresses seed emergence and early seedling growth, with toxicity intensifying as urea levels increase [30,31]. Consequently, the elevated ammonia levels in the 4 N treatment likely exerted potent phytotoxicity, serving as the primary factor in the observed reduction of emergence performance.

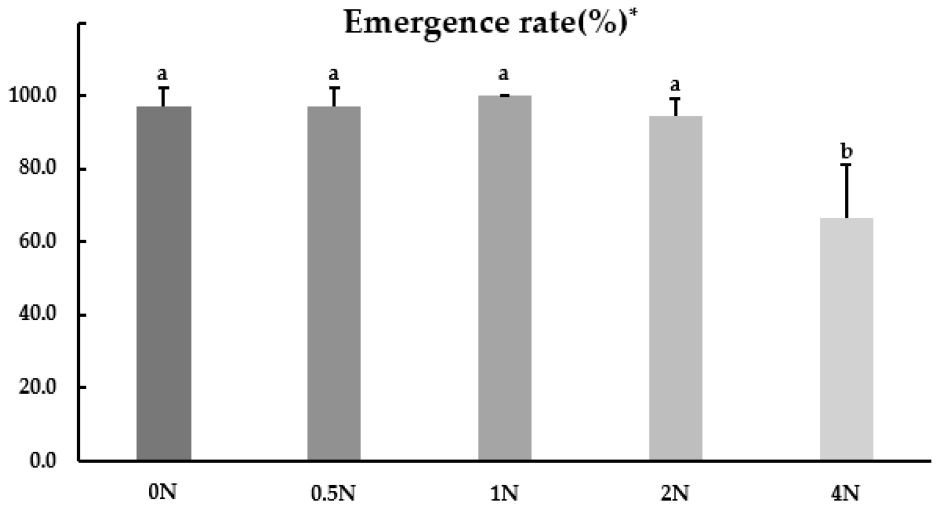


Figure 2. Effect of treatment concentration on emergence rate. Note: Data are presented as means (n = 3 plots per treatment, with 12 plants per plot). Particularly for emergence rate and certain growth parameters, the Aligned Rank Transform (ART) was performed because these data violated the assumptions of normality and homogeneity of variance. Following the ART, different letters (a, b) and asterisks (*) indicate statistically significant differences among all treatments and between the other treatments and 4N treatment, respectively ($p < 0.05$), based on Fisher's LSD post hoc test.

Urea top-dressing significantly promoted elongation and biomass accumulation in both roots and shoots across all growth stages (25, 40, and 70 DAS) compared to the 0 N control (Table 4). At 70 DAS, root length showed a significant declining trend at the 4 N level; however, no statistically significant differences were observed in root diameter, shoot biomass, or root biomass among the fertilized groups, except for the control. The high Shoot to Root (S/R) ratio observed in the 0 N treatment during the early growth stage (25 DAS) is attributed to the extreme limitation of root development due to nitrogen deficiency compared to the fertilized treatments. Although the disparity in S/R ratios among treatments diminished toward the harvest stage likely due to the gradual nutrient release from the basal compost and the internal physiological balancing mechanisms the fact that the biomass of the 0 N treatment at harvest reached only approximately 30% of the average of the fertilized groups (0.5–4 N) underscores the critical importance of nitrogen fertilization in radish cultivation [32]. Notably, while the 4 N level recorded the highest root biomass among all treatments, it also induced physiological disorders such as branching and root cracking (Figure A2). This aligns with previous findings that excessive nitrogen supply triggers excessive vegetative growth in horticultural crops, leading to physiological disorders such as reduced yield, lower fruit set, and impaired floral bud formation [33–35]. In conclusion, consistent with prior studies, an application of 0.5 N level was sufficient to achieve optimal growth efficiency [28]. However, to address the issue of crop non-uniformity caused by large variance (SE = ±209.2 g in fresh root weight), further detailed research is required to refine fertilizer management and enhance nitrogen use efficiency.

Table 4. Effects of different urea application rates on root morphology and biomass distribution of radish at various growth stages.

Growth Stage	Treatment Levels	Root Length (cm)	Root Diameter (cm)	Fresh Shoot Weight (g/Plant)	Fresh Root Weight (g/Plant)	Shoot Root Ratio
Post first Top-dressing (25 DAS)	0 kg urea ha^{-1}	12.7 ± 1.3 ^{ab}	0.43 ± 0.1 ^{c}	9.4 ± 2.3 ^{b}	0.5 ± 0.2 ^{c}	22.94 ± 6.71 ^{a}
	117 kg urea ha^{-1}	16.2 ± 1 ^{a}	1.67 ± 0.1 ^{ab}	38.5 ± 4.2 ^{a}	9.8 ± 1.4 ^{ab}	7.84 ± 0.53 ^{b}
	234 kg urea ha^{-1}	16.8 ± 1 ^{a}	2 ± 0.1 ^{a}	51.7 ± 3.6 ^{a}	14.1 ± 1.3 ^{a}	5.24 ± 0.08 ^{b}
	468 kg urea ha^{-1}	16.2 ± 1.2 ^{a}	1.47 ± 0.3 ^{b}	48.8 ± 5.1 ^{a}	10.2 ± 2.7 ^{ab}	4.04 ± 0.86 ^{b}
	936 kg urea ha^{-1}	11.2 ± 1.7 ^{b}	1.47 ± 0.1 ^{b}	46.5 ± 5.4 ^{a}	6.5 ± 1.7 ^{b}	3.68 ± 1.49 ^{b}
Significance		*	***	***	**	**
Post second Top-dressing (40 DAS)	0 kg urea ha^{-1}	16.5 ± 1.3 ^{c}	2.77 ± 0.3 ^{b}	41.3 ± 10.8 ^{b}	28.5 ± 7.7	1.54 ± 0.26
	117 kg urea ha^{-1}	22.3 ± 1.3 ^{ab}	5.13 ± 0.1 ^{a}	170.88 ± 50.8 ^{a}	205.9 ± 33.2	1.37 ± 0.17
	234 kg urea ha^{-1}	23.7 ± 1.3 ^{a}	5.63 ± 0.6 ^{a}	207.52 ± 23.3 ^{a}	250.9 ± 60.0	1.15 ± 0.17
	468 kg urea ha^{-1}	20.3 ± 2.7 ^{abc}	5.17 ± 0.2 ^{a}	224.2 ± 23.0 ^{a}	195.3 ± 25.2	0.91 ± 0.08
	936 kg urea ha^{-1}	16.9 ± 1.5 ^{bc}	5.67 ± 0.9 ^{a}	228.57 ± 34.9 ^{a}	208.6 ± 83.8	0.79 ± 0.35
Significance		*	*	**	ns	ns
Harvest (70 DAS)	0 kg urea ha^{-1}	25.8 ± 1.3 ^{c}	7.4 ± 0.5 ^{b}	65.7 ± 14.1 ^{b}	406.3 ± 74.5 ^{b}	0.16 ± 0.01
	117 kg urea ha^{-1}	34.3 ± 1.2 ^{a}	10.1 ± 0.4 ^{a}	248.7 ± 60.1 ^{a}	1338.1 ± 209.2 ^{a}	0.18 ± 0.02
	234 kg urea ha^{-1}	33.0 ± 1.2 ^{ab}	10.3 ± 0.3 ^{a}	250.6 ± 60.8 ^{a}	1327.9 ± 60.8 ^{a}	0.19 ± 0.02
	468 kg urea ha^{-1}	32.3 ± 2.0 ^{ab}	10.5 ± 0.3 ^{a}	217.1 ± 20.5 ^{a}	1246.4 ± 28.1 ^{a}	0.18 ± 0.02
	936 kg urea ha^{-1}	30.2 ± 1.33 ^{b}	11.0 ± 0.67 ^{a}	273.9 ± 29.3 ^{a}	1595.3 ± 273.2 ^{a}	0.18 ± 0.02
Significance		***	***	***	***	ns

Note: Values are presented as means ± standard error (n = 3 independent plots per treatment). At 25 and 40 DAS, one plant was randomly sampled from each plot (total n = 3 per treatment). At 70 DAS, three plants were randomly sampled per plot and averaged (total n = 9 per treatment). Data were analyzed using one-way ANOVA, and different letters within a column for each growth stage indicate significant differences according to Duncan's Multiple Range Test (DMRT) at $p < 0.05$. Significance levels: ns, not significant, *, $p < 0.05$, **, $p < 0.01$, ***, $p < 0.001$.

3.2. OJIP Transients and Phenomenological Energy Fluxes in Radish Under Heat Stress as Affected by Urea Application Levels

3.2.1. Nitrogen Imbalance Heightens Radish Sensitivity to Heat Stress(21–27 DAS)

At 21 DAS, while the maximum temperature remained below 30 °C (Figure 1), no significant signs of heat stress were observed in the ΔV_{OP} curves (Figure 3a). However, the maximum fluorescence in nitrogen-deficient (0 N) and over-fertilized (4 N) treatments was significantly lower than the standard fertilization group (1 N) (Table 5). This indicates a latent physiological stress induced by nitrogen imbalance even before the high-temperature stress. Nitrogen deficiency typically reduces photosynthetic performance across various crops (maize, tea, and peanut) [36–38], while excessive nitrogen can induce leaf toxicity and increased mesophyll cell density, which restricts CO_2 diffusion into the cells, thereby decreasing the overall photosynthetic rate [39]. Consistent with the OJIP transients, the phenomenological energy flux already reflected the impact of nitrogen imbalance before the onset of thermal stress. At 21 DAS, the ABS/CS, TR_o/CS, and RC/CS in the 0 N and 4 N treatments were approximately 10% lower than those in the 1 N group. These reductions indicate that the capacity for light absorption and energy trapping was already being constrained by nutritional status prior to the heat wave (Figure 4a).

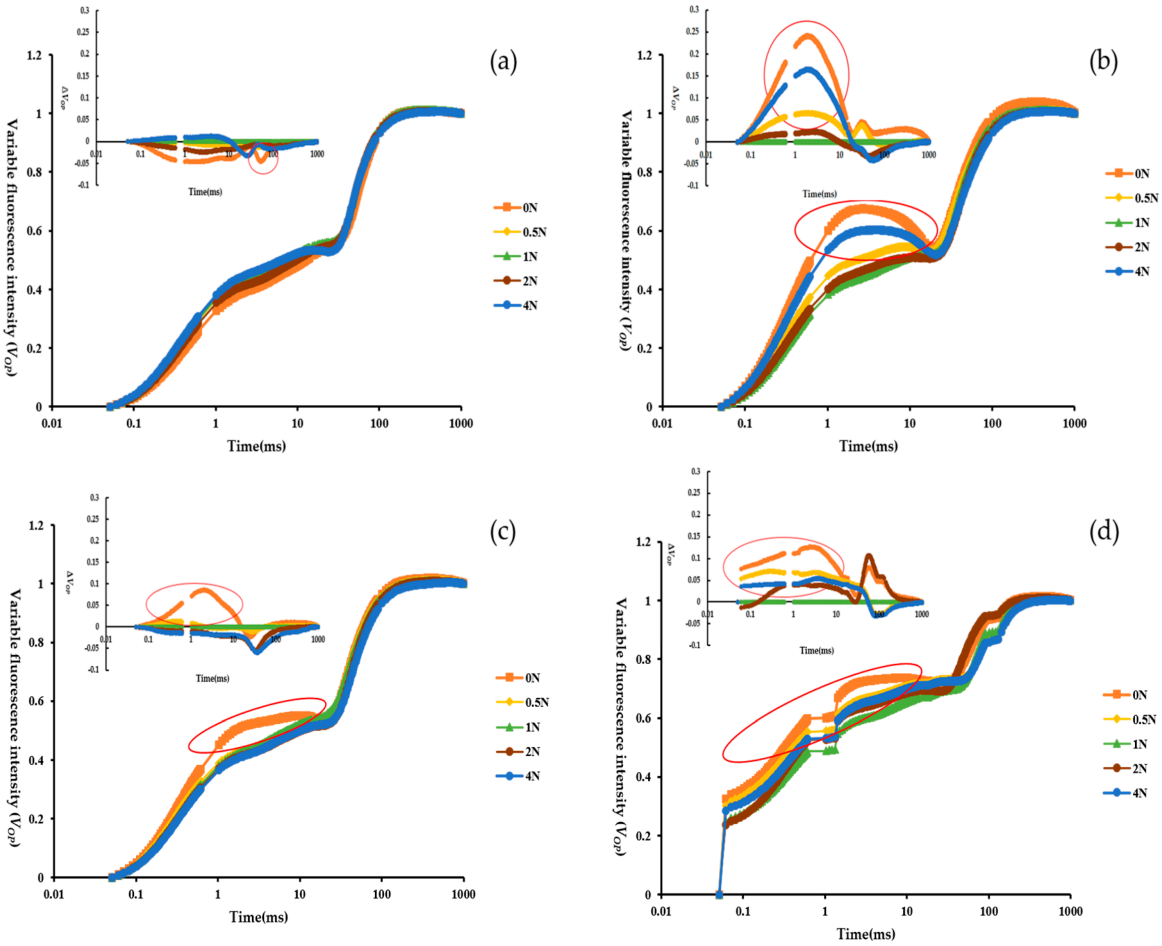


Figure 3. Analysis of photochemical efficiency under heat stress as affected by urea levels at (**a**) 21 DAS, (**b**) 27 DAS, (**c**) 39 DAS, and (**d**) 48 DAS. Note: The 1 N treatment (Standard nitrogen) served as the reference control (baseline at 0). The differences in the O-P transition were visualized using ΔV_{OP} curves, calculated as $\{V_{OP(\text{treatment})} - V_{OP(1\,\text{N})}\}$, where $V_{OP} = (F_t - F_o)/(F_p - F_o)$. Each point represents the mean of six independent leaf measurements ($n = 6$). The red circles highlight the prominent increase in fluorescence intensity at the J-step (2 ms), which indicates a bottleneck in the electron transport chain from Q_A to Q_B.

Table 5. Impact of Nitrogen Application Rates on Photosynthetic Efficiency of Radish under Heat Stress.

Treatment	21 DAS		27 DAS Heat Stress		39 DAS Recovery		48 DAS Heat Stress	
	V_j ns	F_m *	V_j ns	F_m ns	V_j ns	F_m ns	V_j ns	F_m ***
0 N	0.384	28,804 ^{c}	0.658	24,069	0.513	26,973	0.564	21,240 ^{bc}
0.5 N	0.425	31,037 ^{abc}	0.496	29,021	0.435	31,622	0.491	20,315 ^{bc}
1 N	0.432	33,497 ^{a}	0.430	28,956	0.429	29,444	0.440	23,257 ^{b}
2 N	0.409	32,771 ^{ab}	0.474	26,745	0.418	28,935	0.486	29,574 ^{a}
4 N	0.444	30,386 ^{bc}	0.602	24,025	0.413	29,281	0.497	19,465 ^{c}

Note: Measurements were performed on the uppermost fully expanded leaves of six randomly selected plants per treatment ($n = 6$). Data were analyzed using one-way ANOVA; different letters within a column at each growth stage indicate significant differences according to Duncan's Multiple Range Test (DMRT) at $p < 0.05$. Significance levels: ns, not significant, *, $p < 0.05$, ***, $p < 0.001$.

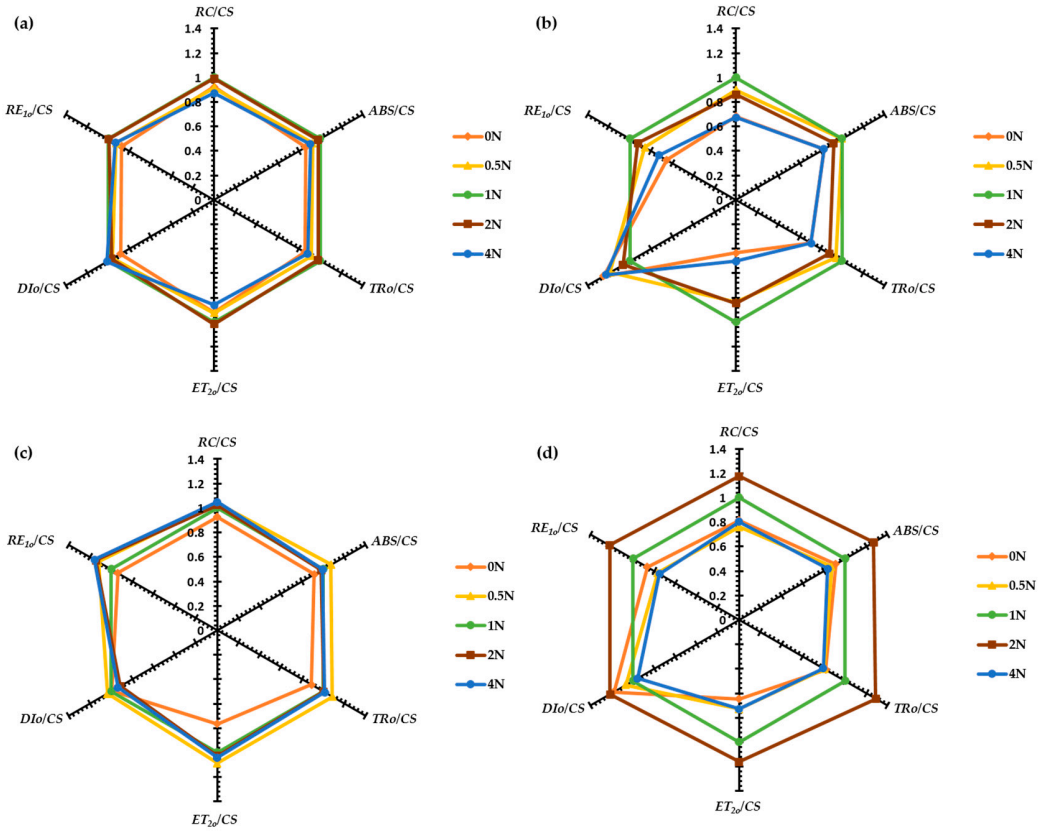


Figure 4. Relative changes in chlorophyll fluorescence parameters compared to the standard nitrogen treatment (1 N) under heat stress at (**a**) 21 DAS, (**b**) 27 DAS, (**c**) 39 DAS, and (**d**) 48 DAS. Note: Photochemical parameters are presented as relative values compared to the 1 N treatment, calculated as: (Treatment)/(1 N treatment). The 1 N treatment (Standard nitrogen) serves as the reference baseline (value = 1). Each point represents the mean of six independent leaf measurements ($n = 6$). The energy fluxes per excited cross-section (*CS*) include: RC/CS (number of active reaction centers), ABS/CS (absorbed energy flux), TR_o/CS (trapped energy flux), ET_{2o}/CS (electron transport flux), RE_{1o}/CS (electron transport flux until PSI acceptors), and DI_o/CS (dissipated energy flux).

Immediately following the first top-dressing at 27 DAS, a sharp increase in temperature occurred, with the maximum reaching nearly 35 °C. OJIP transient analysis during this period showed that extreme heat stress increased individual variability, which limited statistical significance; nonetheless, clear physiological trends were observed. Specifically, a sharp rise in the O-J phase was observed in the 0 N treatment, followed by the 4 N, 0.5 N, and 2 N treatments (Figure 3b). An increase in the O-J phase signifies a bottleneck in the redox process from Q_A to Q_B within the photosynthetic electron transport chain [40,41]. The resulting accumulation of reduced Q_A impairs electron transport toward PSI acceptors [22]. These observations are consistent with previous findings in tomato plants, where nitrogen imbalance was shown to aggravate the O-J phase rise under heat stress, indicating a reduction in the energy connectivity of PSII and an impaired electron flux transfer to the plastoquinone (PQ) pool [42]. The sharp rise was clearly mirrored in the phenomenological energy flux patterns at 27 DAS. In the 0 N and 4 N treatments, the surge in the J-step was accompanied by a severe decline in RC/CS (approximately 30%), which subsequently dragged down both ABS/CS and TR_o/CS. The impact on electron transport was even more pronounced, the electron transport flux (ET_{2o}/CS) representing the heat-vulnerable PSII system [43], plummeted by nearly 50%. In contrast, the flux toward PSI acceptors (RE_{1o}/CS), which is known to be relatively more thermostable, fell by approximately 30% [44]. This differential decline suggests that while high-temperature

stress impaired the entire electron transport chain, the primary damage was centered on the PSII reaction centers. Consequently, energy dissipation as heat (DI_o/CS) increased by about 20%, indicating a significant loss of absorbed energy that could no longer be processed through the electron transport chain. In contrast, the 0.5 N and 2 N treatments exhibited much higher buffer capacity. In these groups, RC/CS and electron transport fluxes declined by only about 10%. This disparity confirms that an appropriate nitrogen supply effectively shields the photosynthetic apparatus against acute high-temperature stress, maintaining relatively stable energy processing even under thermal strain. These results suggest that when heat-sensitive radishes are exposed to extreme temperatures, nitrogen nutrient imbalance exacerbates damage to the photosynthetic apparatus, thereby inhibiting electron transport efficiency.

3.2.2. Restoration of Photosynthetic Efficiency and PSII System Depending on Urea Application Levels (39 DAS)

At 39 DAS, as max temperatures stabilized below 30 °C, the photosynthetic apparatus of the 0.5 N, 2 N, and 4 N treatments showed clear signs of restoration, with the electron transport system returning toward its previous levels (Figure 3c). This recovery was supported by the role of nitrogen in facilitating efficient heat dissipation, thereby mitigating damage from energy overload [45]. In these treatments, the phenomenological energy flux patterns exhibited a normalization of energy flow, reflecting the successful stabilization of the PSII system (Figure 4c).

In contrast, the 0 N treatment failed to achieve full restoration of the photochemical machinery despite a slight recovery trend compared to the extreme heat period. Even under stable temperatures, the electron transport flux (ET_{2o}/CS) in the 0 N group remained 24% lower than that of the 1 N treatment. This lack of resilience can be attributed to an insufficient nitrogen supply, which is indispensable for the resynthesis of damaged core proteins, such as D1, and the restoration of active reaction centers [15,16,42,46,47]. The persistence of this damage was further demonstrated by the ΔV_{OP} curves, where the J-step remained elevated in the 0 N treatment (Figure 3c), indicating a chronic bottleneck in the electron transport chain that could not be resolved without adequate nitrogen supplementation.

3.2.3. Effects of Extreme Heat Stress and Cumulative Nitrogen Imbalance on Photosynthetic Efficiency of Radish (48 DAS)

At 48 DAS, the OJIP transient curves deviated significantly from the typical shape, confirming that all treatments were subjected to extreme high-temperature stress (Figure 3d). Compared to the 1 N control, the 0 N, 0.5 N, and 4 N treatments exhibited a simultaneous rise in both the J-step and the K-step (≈300 µs) on the ΔV_{OP} curves. This simultaneous rise indicates not only a bottleneck in electron transport following Q_A reduction but also damage to the oxygen-evolving complex (OEC) responsible for water photolysis [22]. Consequently, the phenomenological energy flux radar charts for these groups showed a collapsed pattern, heavily skewed toward energy dissipation as heat (DI_o/CS), indicating a functional breakdown of the photosynthetic machinery (Figure 4d). Furthermore, the significant reduction in Fm in the 0 N, 0.5 N, and 4 N treatments compared to the 2 N group further underscores the functional impairment of the photosynthetic machinery.

In contrast, the 2 N treatment maintained a robust hexagonal radar chart, approximately 20% more expanded than the 1 N group, and recorded the highest maximum fluorescence and electron transport efficiency. These results suggest that under cumulative extreme stress, a nitrogen supply moderately higher than the standard (1 N) is more effective in stabilizing PSII and maximizing photoprotection. We hypothesize that the 2 N level enhances protective mechanisms, potentially by facilitating heat shock protein

(HSP) synthesis through its more abundant nitrogen resources. Although HSPs were not directly quantified, previous research indicates that their production, critical for PSII stability under heat, entails a substantial nitrogen cost, and sufficient N availability enhances chloroplast HSP accumulation [15]. Notably, the 4 N treatment failed to provide similar benefits despite high nitrogen availability. This suggests that excessive nitrogen application may induce physiological toxicity or nutrient imbalances that outweigh potential photoprotective advantages, leading to a loss of resilience under sustained stress.

3.2.4. Decoupling of Physiological Resilience and Final Root Yield

The physiological resilience observed at the 2 N level did not translate into a significant increase in final root yield. Similar findings in maize suggest that yield levels and nitrogen responses are often independent, being heavily influenced by unpredictable weather patterns and environmental variability [48,49]. Factors such as N mineralization and in-season climatic shifts create significant spatial and temporal variability in yield [50]. In this study, while the 2 N supply stabilized the photosynthetic apparatus, environmental factors during root enlargement likely decoupled this resilience from final biomass. Specifically, extreme temperature fluctuations may have impaired photoassimilate translocation from leaves to storage roots. This suggests that the optimal N rate for photosynthetic stability may not necessarily align with the rate required for maximizing yield under stressful conditions.

4. Conclusions

This study demonstrates that nitrogen (N) supply significantly modulates the photosynthetic resilience of radish under high-temperature stress. A high level (2 N) proved most effective in maintaining PSII structural stability and enhancing photoprotective mechanisms. However, this physiological advantage did not translate into proportional yield gains, as no significant biomass differences were observed between 0.5 N and 2 N treatments. These findings suggest that enhanced photoprotection alone does not guarantee increased yield under heat stress, likely due to altered carbon partitioning or elevated metabolic maintenance costs. From an agronomic perspective, these findings suggest that in the face of increasing climatic instability, fertilization strategies must evolve beyond a singular focus on yield maximization toward a more comprehensive approach that accounts for diverse environmental constraints. Notably, analysis of cumulative nitrogen load by stage revealed that the total nitrogen in the 0.5 N treatment was lower than even the cumulative 1 N dosage at the first top-dressing stage (159 kg urea ha^{-1}). This deficiency appears to have restricted the acquisition of metabolic resources essential for safeguarding the photochemical apparatus, thereby compromising the buffering capacity against environmental stress and leading to high yield variability ($SE = \pm 209.2$ in fresh root weight). Conversely, the 4 N treatment (336 kg urea ha^{-1}) exceeded the total 1 N dosage (234 kg urea ha^{-1}) as early as the basal fertilization stage, where early-stage toxicity, including impaired emergence and stunted initial growth, offset any potential physiological benefits.

Consequently, rather than simply increasing nitrogen inputs, identifying an optimal balance point is paramount for sustainable agriculture. Fine-tuning nitrogen application around the conventional 1 N level offers a pragmatic compromise between physiological resilience, yield stability, and the reduction of environmental runoff. Furthermore, future precision fertilization strategies must evolve beyond simple total quantity adjustments toward optimizing fertilization timing and split application ratios in direct conjunction with growth stage-specific stress forecasts. By evaluating nitrogen optimization under multifaceted stress scenarios, such approaches will contribute to the development of highly

precise, climate-resilient fertilization strategies that prioritize crop stability in an era of unpredictable weather patterns.

Author Contributions: Conceptualization—S.Y.Y., T.W.K.; Methodology—T.S.E.; Validation—T.W.K., S.Y.Y., and T.W.K.; Investigation—T.S.E.; Resources—T.S.E.; Writing—original draft preparation—T.S.E.; Writing—review and editing—T.S.E., S.Y.Y., and T.W.K. All authors have read and agreed to the published version of the manuscript.

Funding: This study was supported by the Korea Institute of Planning and Evaluation for Technology in Food, Agriculture and Forestry (IPET) through the Agriculture and Food Convergence Technologies Program for Research Manpower development, funded by the Ministry of Agriculture, Food and Rural Affairs (MAFRA) (RS-2024-00400922).

Data Availability Statement: The original contributions presented in the study are included in the article, further inquiries can be directed to the corresponding authors.

Conflicts of Interest: The funders had no role in the design of the study, the collection, analyses, or interpretation of data, the writing of the manuscript, or the decision to publish the results.

Abbreviations

OEC	Oxygen-evolving complex
N	Nitrogen
HSPs	Heat shock proteins
OJIP	Origin Jump Intermediate Peak
PSII	Photosystem II
PI	Performance indices
CRD	Completely randomized design
DAS	Days after sowing
SWC	Soil water content
SE	Standard error
ROS	Reactive oxygen species

Appendix A

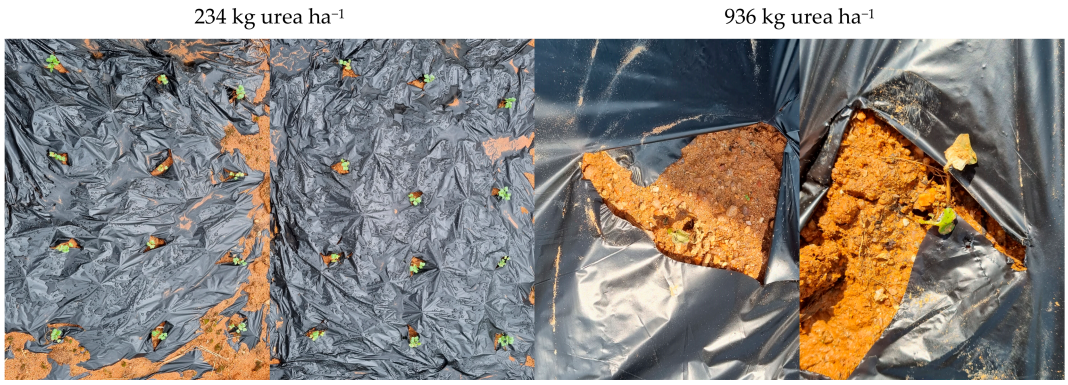


Figure A1. Comparative observation of seedling vigor between 1 N (Standard) and 4 N (excessive) nitrogen levels.

Equation (A1): Calculation of Ammonia Emission Rate

$$ER = Q(C_e - C_i)W_m T_{std} P_a / 10^6 V_m T_a P_{std} \times 10^3 \quad \text{(A1)}$$

ER: emission rate (mg min^{-1}). Q: Airflow rate into the chamber (L min^{-1}). C_e: gas concentration of air leaving the chamber (mg kg^{-1}). C_i: gas concentration of air entering

the chamber (mg kg^{-1}). W_m: Molecular weight of the gas (g mol^{-1}). V_m: molar volume at standard temperature (0 °C) and pressure (101.325 kPa), 22.4 L mol^{-1}. T_{std}: standard temperature, 273.15 K. T_a: temperature of the sample air, K (273.15 + sample air °C). P_{std}: standard pressure, 101.325 kPa. P_a: local barometric pressure, kPa.



Figure A2. Physiological disorders of radish roots induced by excessive nitrogen (4 N level).

References

1. Akram, N.A.; Noreen, S.; Noreen, T.; Ashraf, M. Exogenous application of trehalose alters growth, physiology and nutrient composition in radish (*Raphanus sativus* L.) plants under water-deficit conditions. *Braz. J. Bot.* **2015**, *38*, 431–439. [CrossRef]
2. Sirtautas, R.; Samuoliene, G.; Brazaityte, A.; Duchovskis, P. Temperature and photoperiod effects on photosynthetic indices of radish (*Raphanus sativus* L.). *Agriculture* **2011**, *98*, 57–61.
3. Zha, L.; Liu, W. Environment; Biotechnology. Effects of light quality, light intensity, and photoperiod on growth and yield of cherry radish grown under red plus blue LEDs. *Hortic. Environ. Biotechnol.* **2018**, *59*, 511–518. [CrossRef]
4. Oh, S.Y.; Moon, K.H.; Shin, M.J.; Lee, S.E.; Koh, S.C. Growth characteristics and productivity of radish (*Raphanus sativus* var. *hortensis*) under different day and night cultivation temperatures. *Korean J. Hortic. Sci. Technol.* **2022**, *40*, 168–178. [CrossRef]
5. Irshad, A.; Rehman, R.N.U.; Kareem, H.A.; Yang, P.; Hu, T. Addressing the challenge of cold stress resilience with the synergistic effect of Rhizobium inoculation and exogenous melatonin application in *Medicago truncatula*. *Ecotoxicol. Environ. Saf.* **2021**, *226*, 112816. [CrossRef]
6. Yang, Z.; Li, W.; Su, X.; Ge, P.; Zhou, Y.; Hao, Y.; Shu, H.; Gao, C.; Cheng, S.; Zhu, G.; et al. Early response of radish to heat stress by strand-specific transcriptome and miRNA analysis. *Int. J. Mol. Sci.* **2019**, *20*, 3321. [CrossRef]
7. Oh, S.; Moon, K.H.; Song, E.Y.; Son, I.-C.; Koh, S.C. Environment; Biotechnology. Photosynthesis of Chinese cabbage and radish in response to rising leaf temperature during spring. *Hortic. Environ. Biotechnol.* **2015**, *56*, 159–166. [CrossRef]
8. Mittler, R. Abiotic stress, the field environment and stress combination. *Trends Plant Sci.* **2006**, *11*, 15–19. [CrossRef]
9. Taiz, L.; Zeiger, E.; Møller, I.M.; Murphy, A. *Plant Physiology and Development*; Sinauer Associates Incorporated: Sunderland, MA, USA, 2015.
10. Gregersen, P.L.; Holm, P.B. Transcriptome analysis of senescence in the flag leaf of wheat (*Triticum aestivum* L.). *Plant Biotechnol. J.* **2007**, *5*, 192–206. [CrossRef]
11. Kamal, N.M.; Gorafi, Y.S.A.; Abdelrahman, M.; Abdellatef, E.; Tsujimoto, H. Stay-green trait: A prospective approach for yield potential, and drought and heat stress adaptation in globally important cereals. *Int. J. Mol. Sci.* **2019**, *20*, 5837. [CrossRef]
12. Hong, M.J.; Kim, D.Y. Recent Advances in Nitrogen Use Efficiency (NUE) Research in Wheat. *Korean J. Breed. Sci.* **2025**, *57*, 251–270. [CrossRef]
13. Lee, K.H.; Lee, K.; Lee, G.; Oh, M.S.; Choi, J.-M.; Im, S.; Jang, S.; Kim, E. Flexible high mobility pentacene transistor with high-k/low-k double polymer dielectric layer operating at-5 V. *Electrochem. Soc. Trans.* **2008**, *16*, 239. [CrossRef]
14. Wang, K.; Zhang, X.; Goatley, M.; Ervin, E. Heat shock proteins in relation to heat stress tolerance of creeping bent-grass at different N levels. *PLoS ONE* **2014**, *9*, e102914. [CrossRef]
15. Heckathorn, S.A.; Poeller, G.J.; Coleman, J.S.; Hallberg, R.L. Nitrogen availability alters patterns of accumulation of heat stress-induced proteins in plants. *Oecologia* **1996**, *105*, 413–418. [CrossRef]
16. Singh, M.; Singh, V.P.; Prasad, S.M. Responses of photosynthesis, nitrogen and proline metabolism to salinity stress in Solanum lycopersicum under different levels of nitrogen supplementation. *Plant Physiol. Biochem.* **2016**, *109*, 72–83. [CrossRef]
17. Bogard, M.; Jourdan, M.; Allard, V.; Martre, P.; Perretant, M.R.; Ravel, C.; Heumez, E.; Orford, S.; Snape, J.; Griffiths, S.J.; et al. Anthesis date mainly explained correlations between post-anthesis leaf senescence, grain yield, and grain protein concentration in a winter wheat population segregating for flowering time QTLs. *J. Exp. Bot.* **2011**, *62*, 3621–3636. [CrossRef]

18. Gaju, O.; Allard, V.; Martre, P.; Snape, J.; Heumez, E.; LeGouis, J.; Moreau, D.; Bogard, M.; Griffiths, S.; Orford, S.J.; et al. Identification of traits to improve the nitrogen-use efficiency of wheat genotypes. *Field Crops Res.* **2011**, *123*, 139–152. [CrossRef]
19. Papageorgiou, G.C.; Govindjee, G. *Chlorophyll a Fluorescence: A Signature of Photosynthesis*; Springer: Berlin/Heidelberg, Germany, 2004; Volume 19. [CrossRef]
20. Zhu, X.-G.; Govindjee; Baker, N.R.; Desturler, E.; Ort, D.R.; Long, S.P. Chlorophyll a fluorescence induction kinetics in leaves predicted from a model describing each discrete step of excitation energy and electron transfer associated with photosystem II. *Planta* **2005**, *223*, 114–133. [CrossRef]
21. Stirbet, A.; Govindjee. On the relation between the Kautsky effect (chlorophyll a fluorescence induction) and photosystem II: Basics and applications of the OJIP fluorescence transient. *J. Photochem. Photobiol. B Biol.* **2011**, *104*, 236–257. [CrossRef]
22. Strasser, R.J.; Tsimilli-Michael, M.; Srivastava, A. Analysis of the chlorophyll a fluorescence transient. In *Chlorophyll a Fluorescence: A Signature of Photosynthesis*; Springer: Berlin/Heidelberg, Germany, 2004; pp. 321–362. [CrossRef]
23. Stirbet, A.; Lazár, D.; Kromdijk, J.; Govindjee. Chlorophyll a fluorescence induction: Can just a one-second meas-urement be used to quantify abiotic stress responses? *Photosynthetica* **2018**, *56*, 86–104. [CrossRef]
24. Boureima, S.; Oukarroum, A.; Diouf, M.; Cisse, N.; Van Damme, P. Screening for drought tolerance in mu-tant germplasm of sesame (Sesamum indicum) probing by chlorophyll a fluorescence. *Environ. Exp. Bot.* **2012**, *81*, 37–43. [CrossRef]
25. Živčák, M.; Olšovská, K.; Slamka, P.; Galambošová, J.; Rataj, V.; Shao, H.-B.; Kalaji, H.M.; Brestič, M.J. Measurements of chlorophyll fluorescence in different leaf positions may detect nitrogen deficiency in wheat. *Zemdirbyste-Agriculture* **2014**, *101*, 437–444. [CrossRef]
26. Hwang, Y.B.; Park, K.S.; Yoo, S.Y.; Kim, T.W. Interplay of Stress Responses in Pear Tree Revealed by Chlorophyll Fluorescence Under Combined Erwinia amylovora Infection and Temperature Stress. *Horticulturae* **2025**, *11*, 1358. [CrossRef]
27. Tao, M.; Bai, X.; Zhang, J.; Wei, Y.; He, Y. Time-series monitoring of transgenic maize seedlings phenotyping exhibiting glyphosate tolerance. *Processes* **2022**, *10*, 2206. [CrossRef]
28. Eom, T.; Kim, T.; Yoo, S. Effects of Nitrogen Fertilizer Application on Growth, Vegetation Indices, and Ammonia Volatilization in Korean Radish (*Raphanus sativus* L.). *Nitrogen* **2025**, *6*, 42. [CrossRef]
29. Jiang, Y.; Deng, A.; Bloszies, S.; Huang, S.; Zhang, W. Nonlinear response of soil ammonia emissions to fertilizer nitrogen. *Biol. Fertil. Soils* **2017**, *53*, 269–274. [CrossRef]
30. Wan, X.; Wu, W.; Li, C.; Liu, Y.; Wen, X.; Liao, Y.J. Soil ammonia volatilization following urea application suppresses root hair formation and reduces seed germination in six wheat varieties. *Environ. Exp. Bot.* **2016**, *132*, 130–139. [CrossRef]
31. Bremner, J. Recent research on problems in the use of urea as a nitrogen fertilizer. *Fertil. Res.* **1995**, *42*, 321–329. [CrossRef]
32. Ågren, G.I.; Franklin, O. Root: Shoot ratios, optimization and nitrogen productivity. *Ann. Bot.* **2003**, *92*, 795–800. [CrossRef]
33. Weinbaum, S.A.; Johnson, R.S.; DeJong, T.M. Causes and consequences of overfertilization in orchards. *HortTechnology* **1992**, *2*, 112–121. [CrossRef]
34. Stefanelli, D.; Goodwin, I.; Jones, R. Minimal nitrogen and water use in horticulture: Effects on quality and content of selected nutrients. *Food Res. Int.* **2010**, *43*, 1833–1843. [CrossRef]
35. Erel, R.; Dag, A.; Ben-Gal, A.; Schwartz, A.; Yermiyahu, U. Flowering and fruit set of olive trees in response to nitrogen, phosphorus, and potassium. *J. Am. Soc. Hortic. Sci.* **2008**, *133*, 639–647. [CrossRef]
36. Guo, P.; Ren, J.; Shi, X.; Xu, A.; Zhang, P.; Guo, F.; Feng, Y.; Zhao, X.; Yu, H.; Jiang, C. Optimized nitrogen application ameliorates the photosynthetic performance and yield potential in peanuts as revealed by OJIP chlorophyll fluorescence kinetics. *BMC Plant Biol.* **2024**, *24*, 774. [CrossRef]
37. Liu, Z.; Gao, J.; Gao, F.; Liu, P.; Zhao, B.; Zhang, J. Photosynthetic characteristics and chloroplast ultrastructure of summer maize response to different nitrogen supplies. *Front. Plant Sci.* **2018**, *9*, 576. [CrossRef]
38. Lin, Z.-H.; Zhong, Q.-S.; Chen, C.-S.; Ruan, Q.-C.; Chen, Z.-H.; You, X.-M. Carbon dioxide assimilation and photosynthetic electron transport of tea leaves under nitrogen deficiency. *Bot. Stud.* **2016**, *57*, 37. [CrossRef]
39. Albornoz, F. Crop responses to nitrogen overfertilization: A review. *Sci. Hortic.* **2016**, *205*, 79–83. [CrossRef]
40. Mihaljević, I.; Lepeduš, H.; Šimić, D.; Vuletić, M.V.; Tomaš, V.; Vuković, D.; Dugalić, K.; Teklić, T.; Babojelić, M.S.; Zdunić, Z. Photochemical efficiency of photosystem II in two apple cultivars affected by elevated temperature and excess light in vivo. *S. Afr. J. Bot.* **2020**, *130*, 316–326. [CrossRef]
41. Guissé, B.; Srivastava, A.; Strasser, R.J. The polyphasic rise of the chlorophyll a fluorescence (OKJIP) in heat stressed leaves. *Arch. Sci.* **1995**, *48*, 10.5169. [CrossRef]
42. Li, C.; Yang, Z.; Zhang, C.; Luo, J.; Jiang, N.; Zhang, F.; Zhu, W. Heat stress recovery of chlorophyll fluorescence in tomato (*Lycopersicon esculentum* Mill.) leaves through nitrogen levels. *Agronomy* **2023**, *13*, 2858. [CrossRef]
43. Apostolova, E.; Dobrikova, A. 23 Effect of High Temperature and UV-A Radiation on the Photosystem II. In *Handbook of Plant and Grop Stress*; Taylor & Francis Group: Abingdon, UK, 2011.

44. Havaux, M.; Greppin, H.; Strasser, R.J. Functioning of photosystems I and II in pea leaves exposed to heat stress in the presence or absence of light: Analysis using in-vivo fluorescence, absorbance, oxygen and photoacoustic measurements. *Planta* **1991**, *186*, 88–98. [CrossRef]
45. Wahid, A.; Gelani, S.; Ashraf, M.; Foolad, M.R. Heat tolerance in plants: An overview. *Environ. Exp. Bot.* **2007**, *61*, 199–223. [CrossRef]
46. De Las Rivas, J.; Barber, J. Structure and thermal stability of photosystem II reaction centers studied by infrared spectroscopy. *Biochemistry* **1997**, *36*, 8897–8903. [CrossRef]
47. Giardi, M.T.; Masojídek, J.; Godde, D.J. Effects of abiotic stresses on the turnover of the D1 reaction centre II protein. *Physiol. Plant.* **1997**, *101*, 635–642. [CrossRef]
48. Bundy, L.G.; Andraski, T.W.; Ruark, M.D.; Peterson, A.E. Long-term continuous corn and nitrogen fertilizer effects on productivity and soil properties. *Agron. J.* **2011**, *103*, 1346–1351. [CrossRef]
49. Scharf, P.C.; Kitchen, N.R.; Sudduth, K.A.; Davis, J.G. Spatially variable corn yield is a weak predictor of optimal nitrogen rate. *Soil Sci. Soc. Am. J.* **2006**, *70*, 2154–2160. [CrossRef]
50. Alesso, C.A.; Martin, N.F. Spatial and temporal variability of corn response to nitrogen and seed rates. *Agron. J.* **2024**, *116*, 897–916. [CrossRef]

Disclaimer/Publisher's Note: The statements, opinions and data contained in all publications are solely those of the individual author(s) and contributor(s) and not of MDPI and/or the editor(s). MDPI and/or the editor(s) disclaim responsibility for any injury to people or property resulting from any ideas, methods, instructions or products referred to in the content.